Computational Studies on the BF_3-Catalyzed Cycloaddition of Furan with Methyl Vinyl Ketone: A New Look at Lewis Acid Catalysis

Martín Avalos,[†] Reyes Babiano,*[,†] José L. Bravo,[†] Pedro Cintas,[†] José L. Jiménez,[†] Juan C. Palacios,[†] and María A. Silva[‡]

Contribution from the Departamento de Química Orgánica, Facultad de Ciencias, Universidad de Extremadura, E−06071 Badajoz, Spain, and Departamento de Química Orgánica, Facultad de Veterinaria, Universidad de Extremadura, E−10071 Cáceres, Spain

reyes@unex.es

Received May 16, 2000

Transition structures for both uncatalyzed and BF_3-catalyzed Diels−Alder reactions involving furan and methyl vinyl ketone have been determined at the hybrid DFT (B3LYP/6-31G*) level of theory. The transition structures are predicted to be relatively concerted and highly asynchronous in all cases. A subsequent bond-order analysis has been carried out at the MP2/6-31G*//B3LYP/6-31G*. The role of the Lewis acid and the origin of the *endo* selectivity have been discussed in terms of the nature and number of interactions present in the four possible transition structures. The partition of the potential energy barrier has also been used to estimate the contributions of the pure deformation energy and the differential interaction between the reaction partners on passing from the ground state to the saddle point. This analysis reveals that the major influence arises from the heterodiene−dienophile interaction instead of that corresponding to a BF_3−dienophile interaction.

Introduction and Background

The Lewis acid catalysis of Diels−Alder (DA) reactions represents one of the most useful variations of this versatile and venerable methodology. Although DA reactions are little influenced by solvent polarity, Lewis acids may exert a strong effect, and the catalyzed reactions are not only faster but also show increased regio- and stereoselectivities over the uncatalyzed reactions.[1]

The search for a plausible rationale of Lewis acid catalysis has been a long-standing problem in DA reactions. The question is of more than purely theoretical interest, as many reactions would probably not have been possible without the Lewis acids. Frontier orbital theory has been a preliminary toehold in accounting for the effect of Lewis acids by complexation, thereby reducing the electron density of one reactant.[2] Refined treatments have also been provided by several semiempirical[3] and ab initio[4] theoretical studies. Much of the difficulty in coming to an ideological consensus has been attributed to the complexity of catalytic models. For this reason, studies have long been focused on boron-catalyzed DA reactions to perform theoretical calculations at a reasonable computational cost. Nevertheless, a handful of new mechanisms have emerged that describe the ternary association of diene−dienophile−catalyst in the transition state, which their developers say accommodate many, if not all, of the experimental results, thus putting to rest much of the debate.

First, credit should be given to Birney and Houk who studied the role of BH_3 for the coupling of 1,3-butadiene with acrolein at the RHF/6-31G*//3-21G* level.[4a] The same reaction was further analyzed by Yamabe and his associates in a paper that discusses the roles of BF_3 and $AlCl_3$ at the RHF/6-31G* and RHF/3-21G* (for the Lewis acid) levels.[4d] Although the latter authors only considered the *s-cis* conformation of the dienophile, their most salient result was the fact that the favored *endo s-cis* transition structure (TS) corresponded to a [2+4] DA process rather than a classical [4+2] pathway. In a recent study, García et al. studied both the uncatalyzed and BF_3-catalyzed DA cycloaddition between 1,3-butadiene and acrolein at the B3LYP/6-31G* calculation level.[4i] Contrary to the RHF level of theory, the density functional theory predicts that the catalyzed reaction proceeds via the *endo s-cis* [4+2] TS instead of a [2+4] inverse electron demand hetero-DA reaction.

[†] Facultad de Ciencias..

[‡] Facultad de Veterinaria..

(1) Carruthers, W. *Cycloaddition Reactions in Organic Synthesis*; Pergamon Press: Oxford, 1990; pp 50−53. (b) Oppolzer, W. In *Comprehensive Organic Synthesis*; Fleming, I., Trost, B. M., Eds.; Pergamon Press: Oxford, 1991; Vol. 5, pp 315−399. (c) Roush, W. R. In *Comprehensive Organic Synthesis*; Fleming, I., Trost, B. M., Eds.; Pergamon Press: Oxford, 1991; Vol. 5, pp 513−550. (d) Santelli, M.; Pons, J.-M. *Lewis Acids and Selectivity in Organic Synthesis*; CRC Press: Boca Raton, 1996.

(2) Fleming, I. *Frontier Orbitals and Organic Chemical Reactions*; Wiley: Chichester, 1976; pp 161−165.

(3) Branchadell, V.; Oliva, A.; Bertran, J. *J. Mol. Struct. (Theochem.)* **1986**, *31*, 117−120. (b) Jursic, B. S.; Zdravkovski, Z. *Tetrahedron* **1994**, *54*, 10 379−10 390. (c) Hunt, I. R.; Rauk, A.; Keay, B. A. *J. Org. Chem.* **1996**, *61*, 751−757. (d) Domingo, L. R.; Picher, M. T.; Andrés, J. *J. Phys. Org. Chem.* **1999**, *12*, 24−30. (e) De la Torre, M. F.; Caballero, M. C.; Whiting, A. *Tetrahedron* **1999**, *55*, 8547−8554.

(4) Birney, D. M.; Houk, K. N. *J. Am. Chem. Soc.* **1990**, *112*, 4127−4133. (b) McCarrick, M. A.; Wu, Y.-D.; Houk, K. N. *J. Org. Chem.* **1993**, *58*, 3330−3343. (c) Jursic, B. S.; Zdravkovski, Z. *J. Org. Chem.* **1994**, *59*, 7732−7736. (d) Yamabe, S.; Dai, T.; Minato, T. *J. Am. Chem. Soc.* **1995**, *117*, 10 994−10 997. (e) Dai, W.-M.; Lau, C. W.; Chung, S. H.; Wu, D.-Y. *J. Org. Chem.* **1995**, *60*, 8128−8129. (f) González, J.; Sordo, T.; Sordo, J. A. *J. Mol. Struct. (Theochem.)* **1996**, *358*, 23−27. (g) García, J. I.; Mayoral, J. A.; Salvatella, L. *J. Am. Chem. Soc.* **1996**, *118*, 11 680−11 681. (h) Venturini, A.; Joglar, J.; Fustero, S.; González, J. *J. Org. Chem.* **1997**, *62*, 3919−3926. (i) García, J. I.; Martínez-Merino, V.; Mayoral, J. A.; Salvatella, L. *J. Am. Chem. Soc.* **1998**, *120*, 2415−2420. (j) Domingo, L. R.; Arnó, M.; Andrés, J. *J. Org. Chem.* **1999**, *64*, 5867−5875.

10.1021/jo000752b CCC: $19.00
Published on Web 09/01/2000

Some calculations of BH_3-catalyzed hetero-DA reactions tend to favor the *exo* BH_3-coordination over the *endo* one.[4h] However, Domingo and co-workers found a tunable effect for the BH_3-catalyzed inverse-electron-demand cycloadditions of nitroethene and substituted ethenes using the B3LYP/6-31G* calculation level.[4j] Inclusion of the Lewis acid catalyst and solvent effects decrease the potential energy barriers and increase the charge-transfer process from the dienophile to nitroethene. With propene as the 2π component, the inclusion of the Lewis acid modifies the *endo*/*exo* stereoselection, with the *endo* orientation being the favorable approach, although for the reaction with vinyl ethers, the *endo* selectivity decreases.

Keay et al. have studied at a semiempirical (AM1) level the effect of Lewis acids in the intramolecular DA reaction of enones and ynones with a furan diene.[3c] Their results provided an explanation based on the general equilibria involving coordination of starting materials with Lewis acids and the relative basicity of the ketone group. These studies also explain why catalytic quantities of Lewis acid are required when the latter preferentially coordinates with the enone of starting material, in other words, the reactant carbonyl is more basic than the product carbonyl group. Once the product−Lewis acid complex is formed, the Lewis acid dissociates from the product and is then able to recomplex with the starting material, thereby shifting the equilibrium toward products. On the contrary, stoichiometric amounts of Lewis acids are required when the catalyst is complexed to the more basic site in the product and does not dissociate. Similar furan-based intramolecular DA reactions were studied by Dolata et al. using the MM2 program to calculate the transition states.[5] Houk and co-workers also considered an empirical force field based on MM2 to evaluate diastereoselection of intramolecular DA cycloadditions, albeit furan dienes were excluded.[6]

Both experimental and semiempirical (PM3) studies have recently been carried out by Whiting and his associates on different boron Lewis acids for the catalyzed DA reaction of cyclopentadiene with a wide range of enones.[3e] These semiempirical calculations, however, were unable to unify theory and experiment, and thus, gas-phase PM3 calculations suggest that BF_3 and *m*-nitrophenylboron difluoride should have similar reactivity. These results are in contrast with the experimental fact that the latter catalyst is more reactive than both BF_3 and phenylboron difluoride and exhibits larger differences in *endo*/*exo* ratios.

Quantitative MO calculations are powerful tools to elucidate the reaction pathways for these synthetically and mechanistically intriguing processes. Developments in computational methodology make the study of pericyclic processes with the highly correlated ab initio methods possible.[7] This paper presents a high-level theoretical study of the BF_3-catalyzed reaction between furan and methyl vinyl ketone (MVK), which is a paradigmatic prototype of the reaction of heteroaromatics with enones. An understanding of the TSs involved will allow the prediction of selectivities and stereochemistry of the reaction and expand the application of this method for the catalysis of slow or symmetry-forbidden pericyclic reactions.

Computational Methods

Calculations were carried out with the GAUSSIAN 94 series of programs.[8] The geometries of reactants, transition structures, and products were fully optimized at the B3LYP level[9] using the standard 6-31G* basis set. Ab initio (MP2)[10] calculations were also carried out with the GAMESS package[11] at the MP2/6-31G*//B3LYP/6-31G* level to estimate the corresponding bond orders. Hereafter, such calculations will be referred to as the DFT and MP2 results. Frequency calculations were performed to characterize the nature of stationary points, including the transition structures, which have only one imaginary frequency, and to determine zero-point energies, enthalpies, and free energies. For the TSs, the vibration associated with the imaginary frequency was checked to correspond with a displacement in the direction of the reaction coordinate.

Results and Discussion

Choice of DFT Methods. Before going any further, it is convenient to make a few preliminary comments about the appropriateness of DFT methods, which have elicited some pros and cons. Most of the research achieved so far claims that this theory has proved to be an economical, yet satisfactory, methodology to incorporate the otherwise key electron correlation effects. From a conceptual viewpoint, however, DFT and MPn-based methods do involve a different type of electronic correlation.[12] The most thorough high level MO studies on DA reactions were on the archaetypical cycloaddition of butadiene and ethylene.[7a] At the B3LYP/6-31G* level, the TS is predicted to be concerted, and the lowest energy stepwise pathway has a free energy of activation 7.7 kcal/

(5) Dolata, D. P.; Harwood, L. M. *J. Am. Chem. Soc.* **1992**, *114*, 10 738−10 746. (b) Parrill, A. L.; Dolata, D. P. *Tetrahedron Lett.* **1994**, *35*, 7319−7322.

(6) Raimondi, L.; Brown, F. K.; González, J.; Houk, K. N. *J. Am. Chem. Soc.* **1992**, *114*, 4796−4804.

(7) Goldstein, E.; Beno, B.; Houk, K. N. *J. Am. Chem. Soc.* **1996**, *118*, 6036−6043. (b) Wiest, O.; Houk, K. N. In *Topics in Current Chemistry, Vol. 183. Density Functional Theory IV: Theory of Chemical Reactivity*; Springer-Verlag: Berlin, 1996; Chapter 1. (c) Whiting, A.; Windsor, C. M. *Tetrahedron* **1998**, *54*, 6035−6050. (d) Jursic, B. S.; Zdravkovski, Z. *J. Chem. Soc., Perkin Trans. 2* **1995**, 1223−1226. (e) Jursic, B. S. *J. Org. Chem.* **1995**, *60*, 4721−4724. (f) Park, Y. S.; Lee, B. S.; Lee, I. *New J. Chem.* **1999**, *23*, 707−715. (g) Karadakov, P. B.; Cooper, D. L.; Gerratt, J. *J. Am. Chem. Soc.* **1998**, *120*, 3975−3981.

(8) Frisch, M. J.; Trucks, G. W.; Schlegel, H. B.; Gill, P. M. W.; Johnson, B. G.; Robb, M. A.; Cheeseman, J. R.; Keith, T.; Petersson, G. A.; Montgomery, J. A.; Raghavachari, K.; Al-Laham, M. A.; Zakrzewski, V. G.; Ortiz, J. V.; Foresman, J. B.; Cioslowski, J.; Stefanov, B. B.; Nanayakkara, A.; Challacombe, M.; Peng, C. Y.; Ayala, P. Y.; Chen, W.; Wong, M. M.; Andres, J. L.; Replogle, E. S.; Gomperts, R.; Martin, R. L.; Fox, D. J.; Binkley, J. S.; Defrees, D. J.; Baker, J.; Stewart, J. P.; Head-Gordon, M.; Gonzalez, C.; Pople, J. A. Gaussian 94, Revision D.1; Gaussian, Inc.: Pittsburgh, PA, 1995.

(9) Parr, R. G.; Yang, W. *Density Functional Theory of Atoms and Molecules*; Oxford University Press: Oxford, 1989. (b) Becke, A. D. *J. Chem. Phys.* **1993**, *98*, 5648−5652. (c) Lee, C.; Yang, W.; Parr, R. *Phys. Rev. B* **1988**, *37*, 785−789. (d) Baerends, E. J.; Gritsenko, O. V. *J. Phys. Chem. A* **1997**, *101*, 5383−5403.

(10) Hehre, W. J.; Radom, L.; Schleyer, P. v. R.; Pople, J. A. *Ab Initio Molecular Orbital Theory*; Wiley: New York, 1986.

(11) Schmidt, M. W.; Baldridge, K. K.; Boatz, J. A.; Elbert, S. T.; Gordon, M. S.; Jensen, J. H.; Koseki, S.; Matsunaga, N.; Nguyen, K. A.; Su, S. J.; Windus, T. L.; Dupuis, M.; Montgomery, J. A. *J. Comput. Chem.* **1993**, *14*, 1347−1363.

(12) *Topics in Current Chemistry, Vol. 180. Density Functional Theory I: Functionals and Effective Potentials*; Nalewajski, R. F., Ed.; Springer-Verlag: Berlin, 1996. (b) *Density Functional Theory*; Gross, E. K. U.; Dreizler, R. M., Eds.; NATO ASI Series B: Physics, Vol. 337; Plenum Press: New York, 1995. (c) For comparative purposes with ab initio methods, see also: Pople, J. A. *Angew. Chem., Int. Ed.* **1999**, *38*, 1894−1902.

Scheme 1

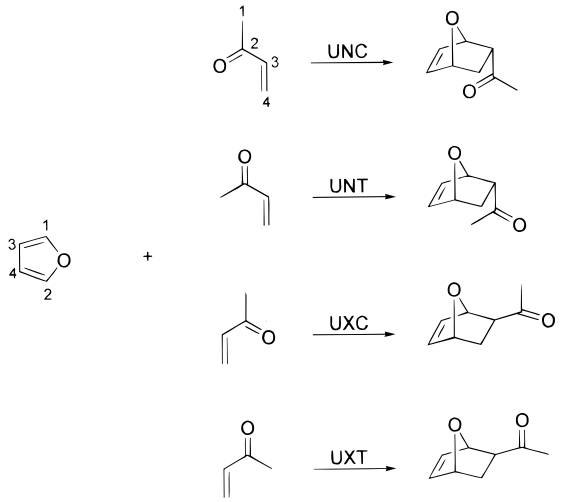

mol above that of the concerted mechanism. Only a calculation at the QCISD(T)/6-31G*//CASSCF/6-31G* level gives results comparable to the hybrid DFT method. In a recent reinvestigation on the same reaction, Lee and co-workers[7f] found that the MP2 results show, in general, the same trend as the DFT calculations in terms of regioselectivity, stereoselectivity, and asynchronicity. Nevertheless, the MP2 correlation energy tends to overestimate the electron correlation effects in the TS, also lowering the activation energy. The latter, together with lower product energies at the MP2 level, results in TSs at a earlier position than the DFT TSs. Moreover, the DFT geometries were more asynchronous than the MP2 TSs. Further studies on a large number of hetero-DA reactions also evidenced that the DFT calculations led to more asynchronous TSs, albeit predicting the same stereochemical and reactivity patterns as the MP2 ones. This accounts for similar electron correlation effects at both levels of theory and justifies the growing use of DFT calculations for DA cycloadditions.

Geometries of the Transition Structures. Four possible TSs can be viewed for the uncatalyzed reaction (U) depending on the approach of the diene with respect to the carbonyl group of the dienophile (*endo*, *exo*) and on the conformational bias of the latter (*s-cis* or *s-trans*).[4a] Scheme 1 displays such orientations, which will be hereafter denoted as UNC, UNT, UXC, and UXT. Similarly, four TSs are also possible for the catalyzed reaction (C) in which the BF_3 coordinates with the carbonyl oxygen atom in a syn disposition with respect to the methyl group of MVK. Such structures will now be referred to as CNC, CNT, CXC, and CXT. All of the DFT TSs for the uncatalyzed reactions correspond to a concerted but asynchronous reaction pathway (Figure 1).

The degree of asynchronicity can easily be viewed in terms of the difference between the bond lengths C1−C3 and C2−C4, which are being formed in the TSs, with the former being the longer bond. We have also found that the *s-cis* TSs were more asynchronous than the *s-trans* TSs, and notably the *endo s-cis* approach (UNC) resulted in the most asynchronous structure.

Concerning the catalyzed process, the TSs were invariably more asynchronous than the uncatalyzed ones. The forming C1−C3 bond is always longer than the C2−C4 bond, which could be a consequence of the enhancement of the π^* orbital polarization of the dienophile (Table 1). Remarkably, the catalyzed TSs CNC and CNT exhibit a similar degree of asynchronicity and both of them were more synchronous than CXC and CXT (Figure 2).

It is also worth noting that the TS of the CNC reaction is characterized by shorter forming bonds with respect to the rest of the TSs, and hence, that TS is relatively late is indicated by the greater degree of progress in bond formation on the reaction coordinate.

Energies of the Transition Structures. The calculated thermodynamic data of these processes are collected in Table 2. The activation energies for the uncatalyzed reaction follow the order UNC < UXC < UXT < UNT, and likewise, the trend for the BF_3-mediated process is CNC < CXC < CXT < CNT. However, higher energy differences were found in the second series. Furthermore, the presence of BF_3 decreases the energy barrier in the range of 8.2−13.9 kcal/mol. This effect, provided by Lewis acid catalysis, has been previously observed on DA reactions[4a,b,h,j] and can be ascribed to a stronger interaction between the $HOMO_{diene}$−$LUMO_{dienophile}$. Table 1 shows the decrease of the $LUMO_{dienophile}$ energy, by ∼1.6 eV for the complex BF_3-MVK, compared with the MVK itself. This fact decreases the $HOMO_{diene}$−$LUMO_{dienophile}$ energy gap, thereby giving rise to a lower energy barrier for the catalyzed process.

There is also a more noticeable change on the energetics for the BF_3-coordinated TSs because the smaller energy barrier corresponds to the more synchronous CNC TS. This situation matches, but is clearly at odds, with the result for the uncatalyzed reaction for which the more stable geometries are the more asynchronous UNC and UXC TSs. The stability of the *s-cis* arrangement either in an *endo* or *exo* approach can be rationalized assuming the effect of the Coulombic stabilization derived from the charge that is being transferred from the furan to the dienophile (Table 3). Such a stabilization is more favorable for those TSs that hold the dienophile in *s-cis* conformation. An analysis of these results shows that the effect is more pronounced for the catalyzed process in which the positive charge of the heterodiene increases by ∼0.16 au.

To rationalize the origin of the decrease in the activation barriers introduced by the complexation with BF_3, it is convenient to dissect the overall activation energies into deformation and interaction energies. This results in a somewhat complicated partition system, which has been previously established.[4i] The major difficulty stems from the fact that the association furan−MVK−BF_3 cannot be computed from its individual components because the dienophile becomes now a metal complex. Accordingly, the difference in energy between such a complex in the ground state and in the TS should be a combination of the deformation energy plus the interaction energy between BF_3 and MVK. Thus, the deformation energy was estimated independently for each fragment of the TS (BF_3, MVK, and furan), then the interaction energy between the ketone and BF_3, and finally the interaction energy involving the latter complex and furan. Scheme 2 highlights the sequence of interactions that have been considered for each approach. The protocol has been accomplished for both the uncatalyzed and the BF_3-catalyzed reactions, and their results are collected in Tables 4 and 5.

As expected for a late TS, CNC shows the largest deformation energy (94.1 kcal/mol). Moreover, the en-

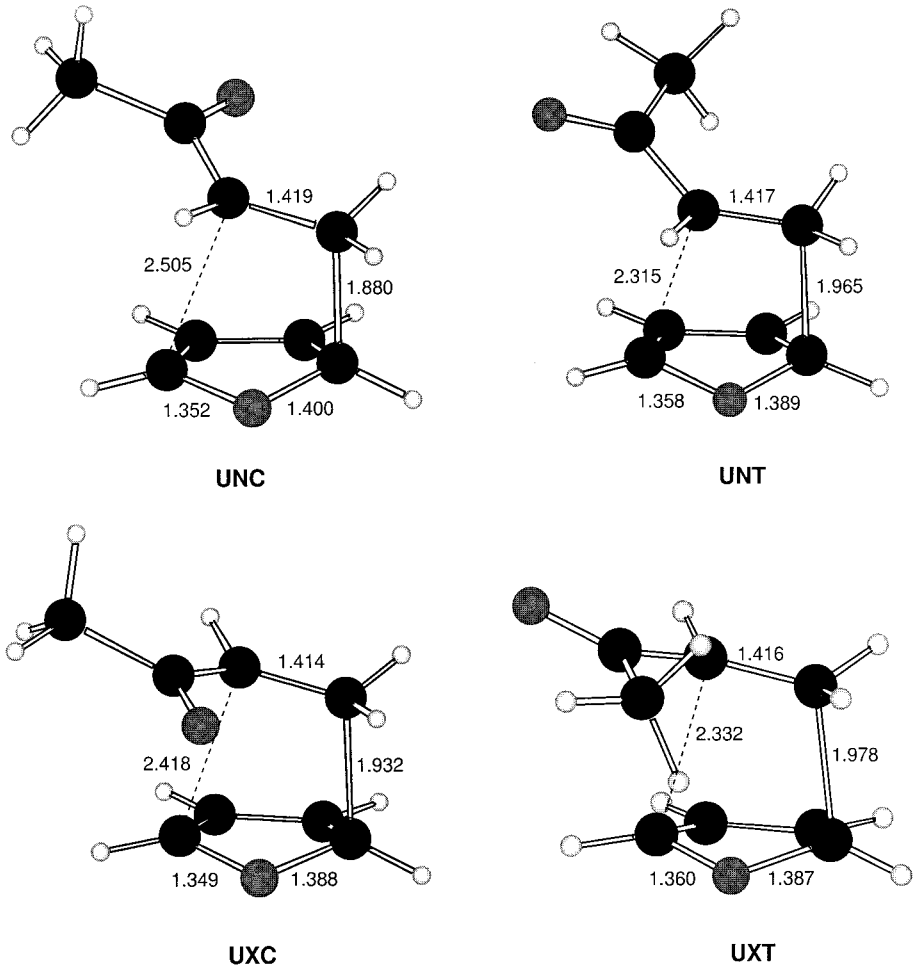

Figure 1. B3LYP/6-31G* transition structures of the reaction between furan and MVK. Bond lengths are given in Å.

Table 1. Frontier Orbital Interactions for Both the Uncatalyzed and the BF_3-Catalyzed Reaction of Furan and MVK at the B3LYP/6-31G* Level

substrate	E^a_{HOMO}	E^a_{LUMO}	C_1	C_2	C_3	C_4
FURAN	−6.095	+0.517	0.38	−0.38	0.23	−0.23
s-cis MVK	−6.721	−1.497	0.04	−0.35	−0.22	0.36
s-trans MVK	−6.748	−1.515	0.01	−0.34	−0.23	0.36
s-cis MVK−BF_3	−8.735	−3.102	0.06	−0.41	−0.15	0.36
s-trans MVK−BF_3	−8.816	−3.048	0.03	−0.40	−0.17	0.35

[a] Values are expressed in eV

hancement of this interaction with respect to the remaining TSs should chiefly be attributed to the deformations of furan and MVK. For the uncatalyzed reaction, however, the deformation energies were found to be similar for all of the TSs, and the most stable UNC TS can be explained in terms of its larger interaction energy.

The decomposition of the interaction energies for the catalyzed process reveals a series of interesting findings. It has been previously suggested that the decrease of the activation energy would come from the enhanced BF_3−dienophile interaction in the TS with respect to the reaction partners.[4i] Aside from this effect, we have found that the interaction of furan−MVK also plays a key role on the selectivity. Similar energies were obtained for the interaction between BF_3 and MVK in the four TSs. This fact is reasonable assuming that the largest contribution to the interaction energy for these components takes place in the first step where the complex BF_3−MVK is formed (−34.9 kcal/mol). It is also interesting to note that the interaction energy between BF_3 and MVK is equally favored (−42 kcal/mol) for the two *s-cis* TSs, CNC and CXC.

With regard to the MVK-furan interaction, there is a significantly higher value (−45.8 kcal/mol) for the CNC TS which gives rise to a lower activation energy for that saddle point. If one considers the interaction energy between fragments **8** and **12** or **9** and **10** of the TS, the same tendency is observed and foremost should be the interaction MVK−furan, common to both fragments. Notably, the interaction between BF_3 and furan (**7**/**9**) becomes even more significant and positive in the case of the CNC geometry (10.5 kcal/mol), albeit the latter does not compensate for the stronger negative interaction between MVK and furan.

Bond Order Analysis and Secondary Orbital Interactions. The relative stability of the *endo* TSs over their *exo* counterparts in the case of the catalyzed process deserves a further examination. The Lewis acid catalyst induces a strong polarization of the dienophile orbitals, thereby altering their energies and giving rise to stronger interactions with the heterodiene. This consideration suggests that the role of secondary orbital interactions (SOI) could play a crucial role in the stereochemical outcome. At first glance, the "classical" SOI, even though they cannot be neglected, would not account for the *endo* selectivity observed, as the CNC TS tends to be at a late position along the reaction coordinate, and therefore, the pair of neighboring components are not forced into such

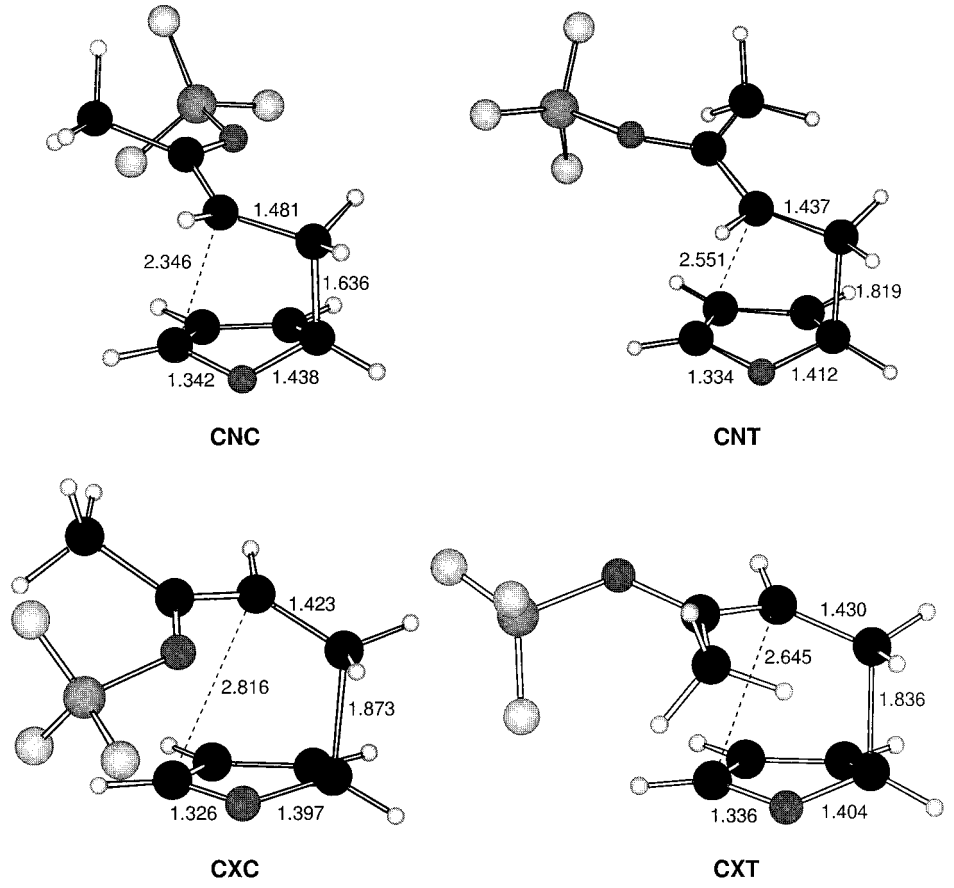

Figure 2. DFT (B3LYP/6-31G*) results for the transition structures for reactions of furan and MVK catalyzed by BF_3. Bond distances are given in Å.

Table 2. Thermodynamic Data (kcal/mol) of the Transition Structures of the Reaction between Furan and MVK, Uncatalyzed and in the Presence of BF_3[a]

TS	$\Delta E^{\ddagger}$	$\Delta\Delta E^{\ddagger}$	$\Delta E_0^{\ddagger}$	$\Delta\Delta E_0^{\ddagger}$	$\Delta H^{\ddagger}$	$\Delta\Delta H^{\ddagger}$	$\Delta G^{\ddagger}$	$\Delta\Delta G^{\ddagger}$
UNC	19.7	0.00	21.0	0.00	20.4	0.00	33.2	0.00
UNT	22.8	3.09	24.4	3.33	23.6	3.14	37.4	4.16
UXC	21.3	1.63	22.8	1.73	22.1	1.66	35.4	2.18
UXT	22.1	2.40	23.7	2.70	22.9	2.49	36.8	3.57
CNC	4.6	0.00	7.8	0.00	6.8	0.00	22.1	0.00
CNT	13.3	8.73	15.7	7.85	15.0	8.25	28.9	6.85
CXC	8.3	3.66	10.6	2.80	10.0	3.22	24.3	2.24
CXT	11.1	6.46	13.5	5.69	12.8	6.03	27.2	5.17

[a] Values are referred to the MVK in its *s-trans* conformation.

Table 3. Mulliken Population Analysis of the Negative Charge (in au) Transferred from Furan to the Dienophile in the TSs

UNC TS	0.16	**CNC TS**	0.31
UNT TS	0.14	**CNT TS**	0.33
UXC TS	0.15	**CXC TS**	0.34
UXT TS	0.14	**CXT TS**	0.32

a close proximity that they present a satisfactory overlap. However, the existence and relative importance of all the possible interactions should anyway be computed.

A quantitative measure of the extent of bond-formation or bond-breaking processes along a given reaction pathway is provided by the estimation of bond order (BO). Traditionally, the latter relates to the valence multiplicity between atoms in a molecule and various definitions of bond order based on quantum mechanical theories have been proposed.[13] This magnitude has also been used to study the molecular mechanism of chemical

Scheme 2

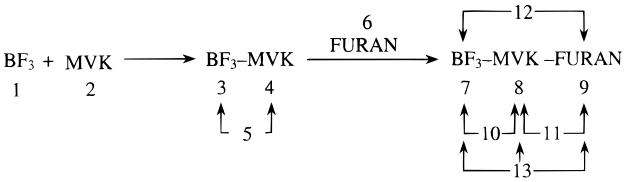

Table 4. Deformation and Interaction Energies (kcal/mol) for the TSs of the Uncatalyzed Reaction between Furan and MVK at the B3LYP/6-31G* Level

	$E_{deformation}$				
TS	FURAN	MVK	total	$E_{interaction}$	$\Delta E^{\ddagger}$
UNC	19.0	13.8	32.8	−13.1	19.7
UNT	21.3	13.3	34.6	−11.9	22.8
UXC	19.6	12.8	32.4	−11.0	21.3
UXT	20.7	12.6	33.3	−11.2	22.1

reactions.[14] Likewise, the bond order uniformity of cyclic chemical systems constitutes an ideal measure of aromaticity.[15]

To follow the nature of the aforementioned DA reactions, the bond indices have been calculated by using the bond order analysis[16] as implemented in GAMESS at the

(13) Pauling, L.; Brockway, L. O.; Beach, J. Y. *J. Am. Chem. Soc.* **1935**, *57*, 2705−2709. (b) Bader, R. F. W. *Atoms in Molecules: A Quantum Theory*; Oxford University Press: Oxford, 1990.

(14) Formosinho, S. J. *J. Chem. Soc., Perkin Trans. 2* **1987**, 61−66. (b) Lendvay, G. *J. Mol. Struct. (Theochem.)* **1988**, *167*, 331−338. (c) Lendvay, G. *J. Phys. Chem.* **1989**, *93*, 4422−4429. (d) Lendvay, G. *J. Phys. Chem.* **1994**, *98*, 6098−6104.

(15) Jursic, B. S. *J. Mol. Struct. (Theochem.)* **1998**, *454*, 105−116.

Table 5. Partition of the Potential Energy Barrier (kcal/mol) for the BF_3-Catalyzed Reaction of Furan and MVK (B3LYP/6-31G* Theory Level)

	$E_{deformation}$				$E_{interaction}$								
TS	BF_3(7)	MVK(8)	FURAN(9)	total	3/4	7/8	8/9	7/9	9/10	7/11	12/8	total	$\Delta E^{\ddagger}$
CNC	27.4	33.0	33.7	94.1	−34.9	−42.3	−45.8	10.5	−58.9	−55.4	−111.7	−101.2	4.6
CNT	28.0	19.6	19.9	67.5	−34.9	−38.9	−10.1	1.9	−26.7	−55.5	−67.5	−65.6	13.3
CXC	29.8	18.5	13.3	61.6	−34.9	−42.9	−4.2	2.2	−21.8	−60.5	−67.0	−64.8	8.3
CXT	29.4	18.6	17.8	65.8	−34.9	−40.3	−7.1	1.4	−26.0	−59.2	−67.7	−66.3	11.1

Scheme 3

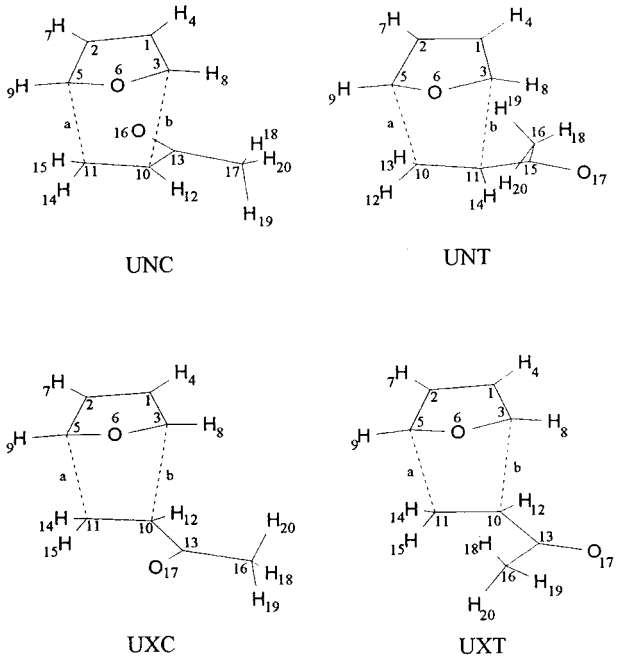

Table 6. Bond Lengths (Å) and Bond Orders at the Transition Structures for the Uncatalyzed and BF_3-Catalyzed Reactions between Furan and MVK

TS	a	b	BO(*a*)	BO(*b*)
UNC	1.880	2.505	0.494	0.248
UNT	1.964	2.314	0.446	0.288
UXC	1.932	2.419	0.459	0.262
UXT	1.979	2.332	0.432	0.284
CNC	1.637	2.346	0.762	0.336
CNT	1.819	2.551	0.552	0.203
CXC	1.873	2.861	0.483	0.128
CXT	1.836	2.645	0.523	0.187

MP2/6-31G*//B3LYP/6-31G* theory level. To aid our discussion below, each atom is numbered in a particular TS for the uncatalyzed reaction (Scheme 3). The same applies to the catalyzed process in which boron and fluoride atoms of the Lewis acid are labeled B21 and F22−F24, respectively.

Bond orders for the "primary" interactions, which are directly involved in carbon−carbon bond-forming reactions, are collected in Table 6. The BO analysis does confirm that the cycloadditions take place via a concerted and asynchronous process where the two σ bonds are simultaneously but dissymmetrically formed. The catalyzed CNC TS affords the greater bond order values, consistent with a later TS. For the uncatalyzed process, however, the BO values (in the range 0.43−0.49 and 0.25−0.29 for each formed bond) indicate a minor change in the asynchronicity and slightly decrease from the *endo* to *exo* approaches.

An examination of additional bond orders are gathered in Tables 7 and 8, either for the uncatalyzed or the catalyzed reaction, respectively. It can be anticipated that the selectivity, based on the energy differences among the four TSs, will largely be dependent on the number and strength of the interactions.

The "crossed" interactions C1−C11 for UNC, UXC, and UXT, even though small (about 0.02), exhibit the higher BO values. In stark contrast, the interaction between C1 and the carbonyl oxygen atom of MVK (O16 for UNC and O17 for the rest of TSs) is negligible. Likewise, the secondary interactions between C1 and the carbonyl carbon atom (C13 for UNC, UXC, UXT, and C15 for UNT) are characterized by their relative weakness.

Interactions with C2 exhibit a similar pattern. Thus, in the case of UNC, UXC, and UXT, there is a significant C2−C10 overlap (0.051−0.077) that corresponds with the interaction C2−C11 for UNT (0.064). Again, the interactions of C2 with the carbonyl atoms of MVK are visible but weak, although in UNC the interaction C2−O16 (0.025) is significantly larger than in the other TSs.

Turning our attention to the catalyzed process (Table 8), the four TSs are characterized by a similar number of interactions. Nevertheless, the dominant interactions C2−C10 (0.065) and C2−O16 (0.029), accompanied by shorter distances, again account for the relative stability of CNC, whereas such interactions are either weaker or nonexistent in the remaining TSs. It should also be pointed out that the important hydrogen bonding type associations between BF_3 and furan (H4−*F*23, H4−F24, or H8−*F*23, H8−F24) depending on the relative geometry of the Lewis acid complex.

Conclusions

The present study demonstrates that DFT calculations at the B3LYP/6-31G* level incorporating electronic correlation constitute an effective and computationally economical tool for describing the model reaction between furan and MVK. As expected from frontier orbital theory, the above calculation predicts a greater asynchronicity of the BF_3-catalyzed transformation with respect to the uncatalyzed reaction, as well as a lower activation energy.

The partition of the potential energy barrier reveals that, for the catalyzed process, the deformation energy for BF_3 is similar in all cases, whereas the major contribution to the overall deformation energy arises from furan and MVK, thereby favoring the CNC approach. Thus, the enhanced interaction energy observed for the CNC TS comes from a prevalent furan-MVK interaction rather than the BF_3-dienophile interaction as found in related Lewis acid-catalyzed DA reactions. The magni-

(16) Mayer, I. *Chem. Phys. Lett.* **1983**, *97*, 270−274. (b) Mayer, I. *Int. J. Quantum Chem.* **1984**, *26*, 151−154. (c) Giambiagi, M. S.; Giambagi, M.; Jorge, F. E. *Z. Naturforsch.* **1984**, *39A*, 1259−1273. (d) Mayer, I. *Theor. Chim. Acta* **1985**, *67*, 315−322. (e) Mayer, I. *Int. J. Quantum Chem.* **1986**, *29*, 73−84.

Table 7. Distances (in Å) and Bond Order Analysis (in Parentheses) of the Transition Structures for the Reaction of Furan and MVK (MP2/6-31G*//B3LYP/6-31G* Theory Level)

TS	C1−C10	C1−C11	C1−C13	C1−C15	C1−O16	C1−O17	C1−H19
UNC	2.947	3.146	3.053		3.130		
	(0.011)	(0.016)	(0.005)		(0.002)		
UNT	3.098	2.885		3.180		3.913	2.865
	(0.022)	(0.008)		(0.002)		(0.002)	(0.005)
UXC	2.874	3.108	3.834			4.516	
	(0.011)	(0.019)	(0.001)			(0.002)	
UXT	2.822	3.092	3.825			4.380	
	(0.009)	(0.022)	(0.002)			(0.002)	
TS	C2−C10	C2−C11	C2−C13	C2−C15	C2−O16	C2−O17	C2−H19
UNC	3.089	2.649	3.406		3.207		
	(0.077)	(−0.010)	(0.006)		(0.025)		
UNT	2.687	3.132		3.716		4.714	2.917
	(−0.005)	(0.064)		(0.003)		(0.008)	(0.007)
UXC	3.079	2.661	4.251			4.751	
	(0.056)	(−0.008)	(0.010)			(0.016)	
UXT	3.076	2.685	4.307			5.122	
	(0.051)	(−0.007)	(0.008)			(0.013)	

Table 8. Distances (Å) and Bond Orders (in Parentheses) of the Transition Structures for the BF_3-Catalyzed Reaction between Furan and MVK at the MP2/6-31G*//B3LYP/6-31G* Level

TS	C1−C10	C1−C11	C1−C13	C1−C15	C1−O16	C1−O17	C1−H19	C2−C10	C2−C11
CNC	2.885	3.072	2.951		2.940			3.013	2.531
	(0.007)	(0.011)	(0.002)		(0.004)			(0.065)	(−0.010)
CNT	3.143	3.005		3.036		3.670	3.335	2.626	3.132
	(0.016)	(0.013)		(0.007)		(0.003)	(<0.001)	(−0.005)	(0.074)
CXC	3.099	3.255	3.687			4.241		3.098	2.676
	(0.016)	(0.017)	(0.001)			(0.003)		(0.045)	(0.001)
CXT	2.956	3.163	3.619			4.039		3.053	2.635
	(0.014)	(0.015)	(<0.001)			(0.003)		(0.049)	(−0.004)
S	C2−C13	C2−C15	C2−O16	C2−O17	C2−H19	H8−*F*23	H8−F24	H4−F24	H4−*F*23
CNC	3.301		2.989						2.367
	(0.017)		(0.029)						(0.039)
CNT		3.478		4.445	3.078			2.557	
		(0.016)		(0.013)	(0.002)			(0.021)	
CXC	4.047			4.499			2.205		
	(0.028)			(0.021)			(0.049)		
CXT	4.059			4.780		2.198			
	(0.031)			(0.020)		(0.065)			

tude of the interaction energy for the CNC TS also justifies most of the decrease in the activation barrier ($\Delta E^{\ddagger} = 6.0$ kcal/mol) on passing from the ground state to the saddle point.

Further examination of primary and secondary interactions reveals that the CNC TS occurs at a relatively late position with the most formed bonds, and that this TS exhibits enhanced interactions between the diene and the vinyl and carbonyl fragments of the dienophile. Globally considered, the Lewis acid complexation appears to facilitate such interactions by bringing atoms close enough to each other during the reaction pathway. The latter also represents a reinforcement of the *endo* rule, which predicts the most stable TS. Forthcoming studies with other relevant DA reaction models, currently under way, will tell us whether the above-mentioned approximation is worthwhile.

Acknowledgment. This work was supported by research funds donated by the Ministry of Education and Culture (Project PB98-0997) and the Junta de Extremadura-Fondo Social Europeo (IPR98-A065 and IPR99-C032). J.L.B. and M.A.S. thank the University and the Junta de Extremadura, respectively, for a fellowship. We are also most indebted to the Servicio de Informática of the University of Extremadura for providing us with its computer facilities. Continuing assistance by Mr. Fernando R. Clemente is gratefully acknowledged.

JO000752B